PRACTICAL IMPLEMENTATION OF THE 3D TETRAHEDRAL TLM METHOD AND VISUALIZATION OF ROOM ACOUSTICS

Stanley J. Miklavcic and Johan Ericsson

Department of Science and Technology
University of Linköping,
S-601 74, Norrköping Sweden
`stami@itn.liu.se`

ABSTRACT

This paper concerns the implementation of a 3D transmission line matrix (TLM) algorithm based on a tetrahedral mesh structure and visualization of room acoustics simulation. Although a well known method, TLM algorithms implemented in 3D are less commonly found in the literature. We have implemented the TLM method using a tetrahedral mesh of pressure nodes with transmission lines lying superimposed on nearest neighbour bonds of a tetrahedral atomic lattice. Results of simulations are compared with those of a standard 3D cartesian mesh and a 2D mesh implementation of TLM. An important feature is a useful graphics interface designed for user-friendly control of room acoustics simulation and visualization in arbitrary shaped rooms containing objects of arbitrary size and number. The paper includes brief discussions of results of using different techniques for modeling totally absorptive or partially absorptive boundaries.

1. INTRODUCTION

Significant effort has been directed to applications of the transmission line matrix (TLM) method in the field of room acoustics simulation. Discussions have focused on topics ranging from the implementation of different boundary conditions [1] to the means of minimizing numerical problems inherent in the discrete TLM approach, such as dispersion effects [2], to means of incorporating boundaries that are not coincident with discrete mesh nodes [3]. The advances made in these directions increase the potential of the TLM method as a method for quantitative study of room acoustics. This is becoming all the more important as computer resources improve and as new areas of application appear. One of the modern areas of application is auralization (the audio counterpart of visualization), in which the artificial reproduction of sound in a simulated environment is accomplished by a convolution of a pure sound signal (representing a given event) and the impulse response of a simulated room. This area of application has a considerable commercial market value for the computer games industry and revolves around coupling realistic audio effects to virtual graphics effects. Naturally, this must be achieved in real-time and must take into account as large a proportion of the frequency spectrum as possible and must also be able to accomodate mobile sources and receivers. These three requirements limit the usefulness of geometric acoustics techniques (such as ray-tracing and beam-tracing [4, 5, 6, 7]). Even though geometric techniques may be quicker to model *early* reflections, the TLM method, with its ability to incorporate full room reverberation effects including interference,

diffraction and frequency effects as well as mobile sources, can represent a potentially viable alternative.

Theoretical studies of the TLM method in terms of defining the quality of acoustic wave reproduction, quantitative accuracy, physical limitations, error analysis, etc, have predominantly been based on the 2D TLM case, either explicitly or with that case implicitly in mind [1, 2, 3, 8, 9, 10]. Furthermore, applications to real systems based on implementation of the 2D TLM method still appear in the literature [11, 12]. Practical examples of 3D implementation are not as prevalent, though some examples can be found [13, 14]. The two strongest reasons for the relatively little effort devoted to 3D TLM modeling are, firstly, the increased simulation time involved with updating a 3D mesh of points and secondly the difficulty of eliciting or extracting information from the 3D results. In this paper we argue that the latter need no longer be a problem with the present availability of computer graphics software, while the former will become less significant with the continuing advance in computer power. Indeed it is now apt to question whether the greater emphasis on 2D simulations should continue. In this paper we discuss two 3D implementations of the TLM method and reflect on their relation to 2D versions.

The obvious generalization to 3D of the most common 2D TLM implementation involves an extension of the square lattice of nodes and equal length transmission lines to a regular cartesian cubic lattice of nodes, each connected to its nearest neighbours by 6 transmission lines. Naturally, this can and does lead to an undesirable increase in computation time. To minimize this increase we have implemented the TLM on an alternate, tetrahedral lattice structure. Here, the 3D array of nodes are once again connected by 4 transmission lines. To justify the numerical effort we rely on the analysis of Van Duyne and Smith III [15, 16] who have, unknown to us at the time of implementation, also considered the notion of a tetrahedral lattice as an alternative and shown that the TLM method on a tetrahedral lattice is locally equivalent to the 3D acoustic wave equation. We compare results of our 3D tetrahedral TLM implementation with those of a 3D cartesian implemented scheme as well as with results of 2D cartesian implementation. We apply our numerical simulation(s) to a realistic model of a concert hall as presented in [12].

2. 3-D TRANSMISSION LINE MATRIX

2.1. Basic Principles

We imagine space to be divided up into a discrete mesh of nodes, each connected with its nearest neighbours by means of digital, bi-
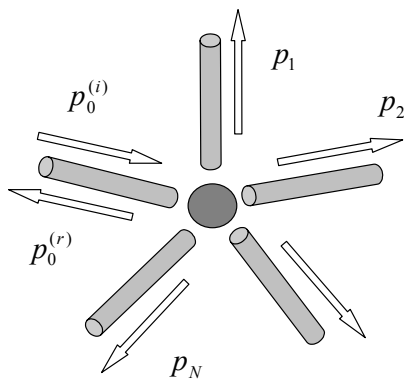
Figure 1: *Schematic of a waveguide junction. Along one of the waveguides, an incident signal, $p_0^{(i)}$, is partially reflected back along the same waveguide, $p_0^{(r)}$, and partially transmitted along the reamining waveguides, p_k.*

directional waveguides. The waveguides allow the transmission of acoustic signals in two directions. At a node several waveguides meet which gives rise to an impedance mismatch between any one of the waveguides and the remainder. This mismatch is a source of reflection at the junction end of the waveguide.

The transport behavior of signals along waveguides and at waveguide junctions can be determined assuming that the cross-sectional dimensions of the waveguides are such that only plane wave signals propagate. The plane wave approximation leads to a simple proportionality relation between acoustic pressure, p, and volume velocity, v, in terms of acoustic impedance, $p/v = \pm Z$, where the positive/negative signs depend on direction.

Suppose we have the general situation depicted in Figure 1.

An input signal along waveguide, 0, meets a junction and experiences a partial reflection. The total pressure along this waveguide is the sum of these two pressure signals, $p_0^{(i)} + p_0^{(r)}$, while the volume velocity is $v_0^{(i)} + v_0^{(r)}$. The partially transmitted energy is divided up into signals which carry along the remaining waveguides, p_j.

The total transported material must be conserved. For a constant density fluid and constant cross-sectional waveguides this gives the condition that the volume velocity must be conserved

$$v_0^{(i)} + v_0^{(r)} = \sum_{j=1}^{N} v_j. \tag{1}$$

Furthermore, the pressures at the junction must be equal

$$p_0^{(i)} + p_0^{(r)} = p_1 = p_2 = \cdots = p_N. \tag{2}$$

This gives rise to the junction pressure relation

$$p_0^{(i)} + p_0^{(r)} = \sum_{j=1}^{N} \frac{p_j}{Z_j} \bigg/ \sum_{j=1}^{N} \frac{1}{Z_j} . \tag{3}$$

The reflection and transmission coefficients for the signal in waveg-

uide 0, are

$$R = \frac{p_0^{(r)}}{p_0^{(i)}} = \frac{\dfrac{1}{Z_0} - \sum_{j=1}^{N} \dfrac{1}{Z_j}}{\dfrac{1}{Z_0} + \sum_{j=1}^{N} \dfrac{1}{Z_j}}, \quad T = 1 - R. \tag{4}$$

For waveguides of identical characteristic impedance these reduce to

$$R = \frac{1 - N}{1 + N}, \quad T = \frac{2N}{1 + N}. \tag{5}$$

For a 2D cartesian mesh with each nodes being the junction for $N + 1 = 4$ equal-impedance waveguides, the pressure transmission coefficient per waveguide, $t = T/N = 1/2$ and the pressure reflection coefficient, $R = -1/2$. For incident waves along all 4 waveguides at junction, K, this result generalizes to a signal transmission described by the scattering matrix,

$$S_{2D} = \frac{1}{2} \begin{bmatrix} -1 & 1 & 1 & 1 \\ 1 & -1 & 1 & 1 \\ 1 & 1 & -1 & 1 \\ 1 & 1 & 1 & -1 \end{bmatrix}, \tag{6}$$

while the total pressure at junction, K, can be expressed as

$$p_K = 2 \sum_{j=1}^{N+1} \frac{p_j^i}{Z_j} \bigg/ \sum_{j=1}^{N+1} \frac{1}{Z_j} . \tag{7}$$

2.2. Boundary Effects

Scattering matrix (6) cannot be used at boundaries. Not only is signal scattering along certain directions prevented, there are different acoustic properties at a boundary. Boundary properties considered here are perfectly reflecting, perfectly absorbing, and partially absorbing-partially reflecting boundaries. In the reflecting cases, only specular reflection is considered for which incoming signals to boundary nodes are returned along the same waveguide with opposite sign (for diffuse reflection one can invoke the ideas of Laird, *et. al.* [3]). With partial absorption we have only used the simple method of multiplying the incident waveguide signal with a reflection coefficient, $\alpha \in [0, 1]$ to obtain the reflected signal traveling back along the same waveguide. This implies use of the matrix

$$S_\alpha = \alpha \begin{bmatrix} -1 & 0 & 0 & 0 \\ 0 & -1 & 0 & 0 \\ 0 & 0 & -1 & 0 \\ 0 & 0 & 0 & -1 \end{bmatrix}.$$

In the case of total absorption we have implemented and tested several methods ranging in complexity. The simplest approach is to set the above reflection coefficient, α, to zero. This is well known to give a good but not ideal representation of absorbing boundary conditions, with ghost reflections prevailing. A second option, Berenger's perfectly matched layer [17, 18], is to surround the physical boundaries with additional layers of nodes each of which behave as a normal interior node except with a scattering matrix $S_\beta = \beta S_{2D}$ with $\beta \in (0, 1)$. This allows signals to extend outside the simulation space, tapering off gradually. We have found this method works well in 2D but becomes prohibitive in 3D due to the significant number of nodes that must be introduced.
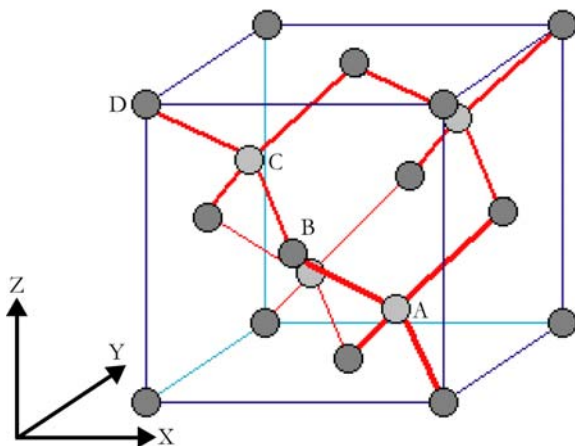
Figure 2: *Tetrahedral lattice*

Finally, we have implemented the Taylor series approximation approach [1], whereby a Taylor series expansion is used to estimate the signal strength to be input into a boundary node, based on signals at neighbouring nodes at previous iterations. We remark that the algorithm as presented in [1] seems best suited to a 2D cartesian mesh, while questions arise as to how to implement the algorithm in 3D, especially for the tetrahedral geometry.

Variations on these themes must be considered for objects existing inside the room itself (*e.g.*, tables, chairs, people, etc.). For example, an absorptive 3D object or even a 2D object (such as a thick heavy curtain) would be difficult to model using the Berenger method which is designed for exterior boundaries (additional sites are introduced outside the simulation space). Here the simplest approach has been taken for all interior cases: use of the scattering matrix, S_α with $\alpha \in [0, 1]$.

2.3. 3D Cartesian Lattice

In 3D the space filling generalization of the 2D square matrix usually employed, involves a 3D array of nodes each connected to nearest neighbors via 6 bi-directional, equal-length waveguides. Apart from the increase in number of nodes, the added effort of shunting signals along the extra waveguides increases the computational demand, thereby decreasing the effectivity of the TLM algorithm. Here, using (5) with $N = 5$, we have $R = -2/3$ and $t = T/N = 1/3$. The scattering matrix for this case of six transmission lines is then a 6×6 matrix, S_{3Dc}, with diagonal elements $R = -2/3$ and off-diagonal elements $t = 1/3$.

2.4. 3D Tetrahedral Lattice

Past experience with 3D space-filling lattice structures [19, 20], has led us to consider the tetrahedral lattice structure of diamond, which has a coordination number of 4. Thus, if the TLM were based on a tetrahedral mesh with waveguide junctions placed on the atomic lattice sites, then each junction or node could be connected to its nearest neighbours via 4 waveguides of equal length. Scattering then again involves (6). This should in priniciple introduce a computational saving compared to the 3D cartesian lattice,

back to the state enjoyed by the 2D simulation. The qualifier that these waveguides are of equal length implies that the signals will be transmitted in along arbitrary waveguides with the same speed. Artificial anisotropy in wavespeed is thus reduced [2, 15, 16, 22]. In addition, comparing the elements of the scattering matrices, S_{2D} and S_{3Dc}, we see that the number of operations involved in the tetrahedral case is also reduced since only division (by 2) is involved as opposed to division (by 3) and multiplication (by -2). Furthermore, division by 2 can be implemented as a right-shift in binary arithmetic [21, 23] with some minor additional computational saving. Finally, to model a given volume requires fewer tetrahedral nodes than cartesian nodes with the same Δl. For example, to model a $1m^3$ box with $\Delta l = 0.01m$, a cartesian mesh requires $1/(0.01)^3 = 1,000,000$ nodes; a tetrahedral mesh requires only $1/((2 \cdot 0.01 \sin(54.45°))^2 (2 \cdot 0.01 \cos(54.45°))) \approx 649,519$ nodes, a saving of roughly a factor of $1/3$.

Taking the waveguide length to be Δl, the positions of the nearest neighbour junctions to a given junction can be determined knowing that the angle between waveguides is $109.5°$. One fact not previously advertised in the literature is the single greatest disadvantage of the tetrahedral mesh. This is that the mesh naturally distinguishes between two different types of nodes, depending on the orientation of their neighbours. In Figure 2 we see that the nearest neighbour directions from node A are (in counterclosewise direction about $z-$axis) $(1, -1, -1), (1, 1, 1), (-1, 1, -1)$ and $(-1, -1, 1)$, while the nearest neighbour directions from node B are $(1, -1, 1), (1, 1, -1), (-1, 1, 1)$ and $(-1, -1, -1)$. The neighbours of node B are rotated $90°$ about the $z-$axis with respect to neighbours of node A. These two node types lie on different planes. Nodes lying on the same plane as node A will bear the same relation to their neighbors as A does to its. This feature repeats every second plane: the plane containing node C is structurally identical to the plane containing node A. Likewise, the plane with node D is identical to the plane with node B. This periodicity can be utilized in the programming of the TLM scattering process by defining two different scattering processes, one for each type of node [23].

As mentioned three possible boundary types: perfectly reflecting, perfectly absorbing (transparent) and partially absorbing were considered. Reflecting and even partially reflecting boundary conditions are sufficiently easy to implement and are quite accurate. For partially reflecting walls, the error associated with ghost reflections are relatively minor compared to the dominating reflected signal strength. For perfectly absorbing walls we have experienced significant complications with our interpretation of Murphy and Howard's scheme [1]. The Taylor series ABC on the tetrahedral lattice did not produce the desired result. We expect that in the original formulation the method relied to some extent on orientation of the boundary: lying parallel to one of the coordinate axes and perpendicular to the other. This is not the situation in our 3D implementation. Work aiming to adapt the idea to the present case is continuing.

2.5. Graphics Interface

One of the difficulties incurred with implementing a 3D simulation is in assessing acoustic information. Simple pressure -vs-time plots associated with specific points in the available 3D space, as we show below, are necessary for a true quantitative analysis. However, these are limited in scope. In particular, it is difficult to know apriori what space points need to be considered for sam-
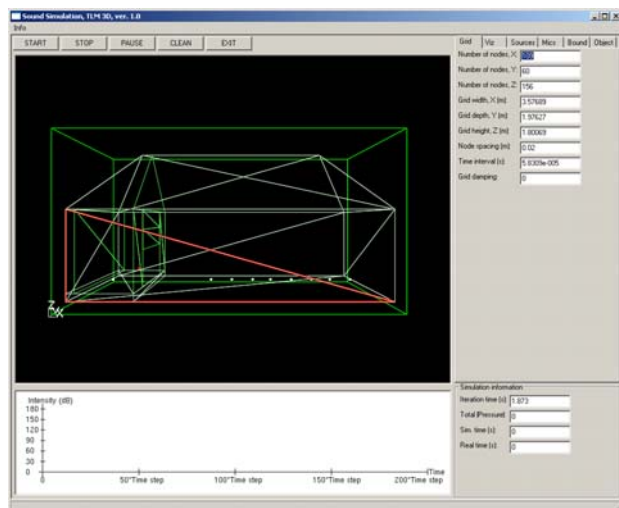
Figure 3: *Screen dump of the final programme's graphical interface. Screen shows the structure inherent in the concert hall model studied by Morton (2001).*

pling of information. This is especially true if the virtual room is complex in shape and totally lacking in symmetry. This problem can be remedied if one is able to visualize the entire acoustic field. Then one can quickly ascertain in which regions interesting phenomena occur and where quantitative focus should be placed. Figure 3 shows a graphic interface we have created in tandem with our TLM simulation [24]. With this interface one can obtain both an overall view of the acoustic field in three dimensions (the large window in the screendump) and quantitative pressure - vs- time plots (lower window) as recorded by any number of virtual microphones positioned in $xyz-$space according to user specifications (data shown either as acoustic pressure in Pa or pressure level in dB). The interface also allows the latter information to be saved as raw data for further audio or analytical processing. In the main window, the room, whose shape and size is specified by the user, can be rotated about any axis through the central point in order to be able to see the acoustic field everywhere - there are no blind spots. Finally, apart from room shape and size, the interface allows the user to introduce arbitrary objects to the room. The surfaces of these objects can be modeled as having any degree of absorption capability from perfectly absorbing to perfectly reflecting. Since the visualization takes a significant fraction of the total simulation time, it is also possible to turn off this feature to speed up the simulation while allowing continued flow of data from the virtual microphones. The latter data can be plotted, saved as raw data or used in audio playback.

This user-friendly interface has the potential to be used for commercial purposes, *e.g.*, by designers and architects in the construction industry, for research by acousticians, as well as for teaching purposes to students of physics and mechanics (studying wave phenomena), engineering (in particular, for acoustic engineering) as well as students of music.[1]

---

[1]This is currently being used at this university for students of media technology and for students of music production.

3. RESULTS

3.1. Comparison of 3D Cartesian and 3D Tetrahedral Meshes

In Section 2.2 we gave reasons for why a saving in computational time would be expected in comparisons between the 3D cartesian and tetrahedral mesh-based TLM modeling. This expectation was realised in all our simulations. As an example, Table 1 shows results of a simple simulation where sound in a rectangular prism shaped room of dimensions $2.0 \times 2.0 \times 1.0$ was simulated using TLM on both 3D cartesian and 3D tetrahedral meshes. In both cases, the nearest neighbour internode distance was kept constant at $0.02\ m$. With or without the added computational cost of visualizing the simulation, the tetrahedral TLM performs considerably faster that the 3D cartesian algorithm, by approximately a factor of 2.[2] This factor also applies to the visualization component, which in relation to total time taken is 25%. The differences in simulation time are mostly due to the fewer number of nodes to be updated, but also the fewer waveguide/node scattering operations to be performed.

	3D Tetrahedral	3D Cartesian
Number of nodes	$313, 200$	$500, 000$
Internode distance (m)	0.02	0.02
TLM iteration time (s)	0.490	0.843
Visualization time (s)	0.121	0.264
Total iteration time (s)	0.611	1.107

Table 1. *Comparison between TLM simulation using cartesian and tetrahedral meshes for a room of size* $2.0 \times 2.0 \times 1.0 = 4.0\ m^3$.

Other comparisons can be found in [23]. More detailed results addressing a quantitative comparison between the tetrahedral 3D model and analytic data for a rectangular geometry will be published elsewhere, as will discussions of spatial dispersion [2, 22].

3.2. 2D -vs - 3D Room Acoustics Simulation - A Practical Example

Clearly, a 2D simulation will not produce the same result as a 3D simulation. A 2D model can be thought of as a 3D model, being infinite in the third dimension, in which case information about the effect of boundaries in this third dimension is lost. A pressure point source in 2D is then re-interpreted as a *line* source in 3D and pressure values are quoted in units of pressure per unit length. Alternatively, a 2D model can be considered when confinement in a given direction is extreme compared with the other two. With either interpretation it is inappropriate to compare directly quantitative 2D and 3D pressures in extended 3D situations. Consequently, quantitative information provided by a 2D simulation is also inappropriate for assessing the acoustic properties of a real world environment. Since 2D simulations are used to study acoustic behavior in 3D systems [11, 12], it is legitimate to even question the relevance of qualitative information produced. We address these issues using a particular case study.

Here, we demonstrate the disparity between 2D and 3D TLM models using the example of a concert hall studied by Morton [12].

---

[2]All calculations were run on a Pentium III 1000 Mhz PC with 512 Mb RAM and 30 Gb ROM. The significance with the information given lies, however, more with the difference in simulation times rather than absolute times.
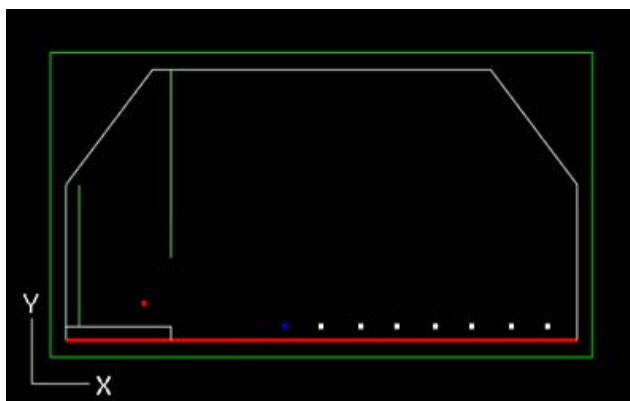
Figure 4: *Screen dump of 2D cross-section of concert hall as modeled by Morton (2001). The red (left most) dot denotes a virtual sound source, remaining points counted 1-8 from left-to-right, denote virtual, pressure-sensitive microphones.*
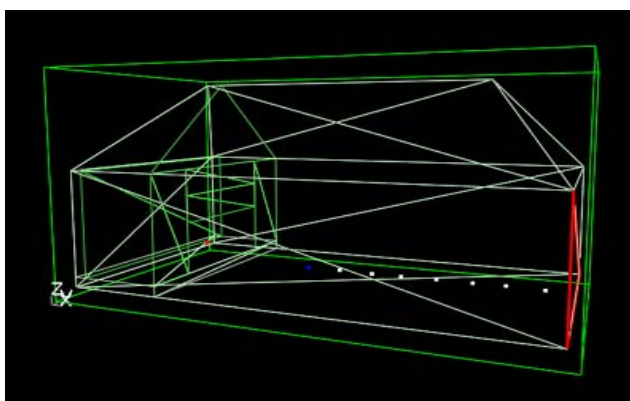

Figure 6: *Comparison of pressure signals as recorded by virtual microphone #3 (18.1, 10.0, 1.9) from 2D and 3D (tetrahedral) simulations. Large amplitude (pink) curve: 2D simulation; low amplitude (black) curve: 3D simulation.*

Figure 5: *Screen dump of full 3D model of concert hall modeled (in 2D) by Morton (2001). The spatial limits in the lateral direction as well as sloping roof/ceiling are clearly seen. Source and virtual microphone positions are as in Figure 4.*

Figure 7: *Comparison of pressure level (dB) as recorded by virtual microphone #3 (18.1, 10.0, 1.9) from 2D and 3D (tetrahedral) simulations. Data is as otherwise given in Figure 6.*

The hall, whose original purpose was as a sports venue, doubles as a concert hall for theatres and musical performances. Morton's simulations aimed at modeling solutions to the inherent acoustic problems of the $34 \times 18 \times 16 \, m^3$ hall. The 2D model of the hall employed by Morton and the true 3D shape of the hall are shown in Figures 4 and 5, respectively. Materials such as wood, fibreboard and concrete are used in its construction and furnishings; the concrete walls are draped by heavy curtains during performances. Relevant acoustic data are provided by Morton [12].

To perform our comparison, Morton's 2D simulations were reproduced by us using information on acoustic and structural features of the concert hall as provided by Morton. Unfortunately, some details (in terms of dimensions, absorption properties, especially of objects in the room) were not provided, which made quantitative comparison between our respective 2D simulations somewhat difficult. Nevertheless, a reasonably accurate reproduction was achieved (see [23] for details). To allow for greater flexibility
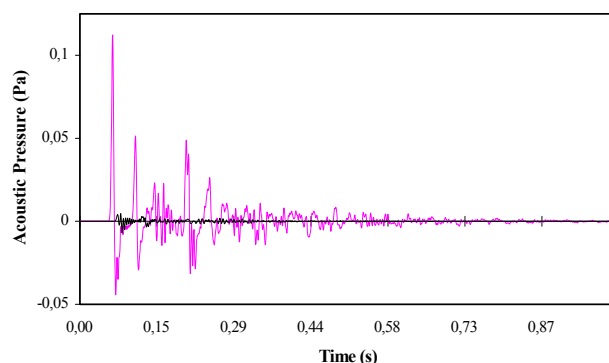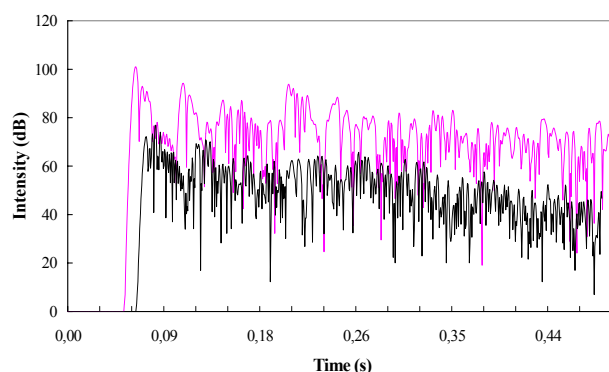
in our comparison between 2D and 3D simulations, we used our own implemented 2D model, rather than rely on data provided by Morton. Times quoted in the figures are based on iteration time (different for 2D and 3D) multiplied by number of iterations.

In both models a Gaussian pulse is sent out from a virtual source placed on a stage fixture. Recordings were made by 8 virtual microphones placed at increasing distances from the stage as shown in Figures 4 and 5. Typical quantitative comparisons of acoustic pressures and pressure levels are shown in Figures 6 and 7. Again, the 2D and 3D magnitudes are not comparable. Overall, the 3D decays much more rapidly than in 2D, as expected. Clearly, 2D models would give a false prognosis of reverberation times for a real structure. With regard to detail, there are few similarities between the results shown in Figures 6 and 7. This is in contrast to a comparison between 2D and 3D simulations of a straight rectangular prism [23]. The simpler geometry there led to more similarly structured curves making for easier identification of contributing reflections (both included and absent in 2D). Here, the more com-

plex geometry with the sloping roof gives rise to a complicated reflection scenario. Only the strong reflections from the back wall of the hall (second strong peaks in Figure 7) and similar ones from the front are discernible.

4. SUMMARY AND CONCLUSIONS

With the continued advance in computer performance we are likely to see an increased usage of room acoustics simulation methods for architectural purposes, music instrument design, as well as the expanding new front of virtual environments. The 2D TLM method has always intimated the potential of TLM as a contender for three dimensional applications. However, in comparison with 2D, 3D acoustic implementations have not been so forthcoming, due partly to a more involved programming task, partly to the increased simulation time and partly the problem of extracting information from a simulation. We have here demonstrated that this potential can indeed be realised in practice by using a judicious choice of discrete mesh and newly available computer graphics methods. Our results confirm the fact that the tetrahedral mesh, despite the inherent programming complexity, is superior to the cubic mesh in terms of computational time as well as total mesh size. 3D visualization adds the dimension of allowing one to see the acoustic field during the simulation and decide where special attention need be directed. 2D TLM models fail to represent real room acoustics for rooms of complex form. They can, however, give some qualitative information for simple box-shaped rooms (data not shown).

Further steps can be taken to improve the performance of the 3D tetrahedral TLM algorithm, primarily by exploiting the natural existence of two interconnecting classes of nodes. It is possible to utilize the two sets of matrices in a parallelized code to speed up computation time. A second important issue is that of the boundary conditions. More efficient approaches, better suited to the current tetrahedral system, must be applied.

5. REFERENCES

[1] Murphy, D. T. and Mullen, J. "Digital waveguide mesh modeling of room acoustics: improved anechoic boundaries" *Proc. 5th Int. Conf. Dig. Audio Effects (DFAX02) Hamburg Germany*, 163-168, 2002.

[2] Savioja, L. and Välimäki, V. "Reducing the dispersion error in the digital waveguide mesh using interpolation and frequency-warping techniques" *IEEE Trans. Speech Audio Proc.*, **8**, 184-194, 2000.

[3] Laird, J., Masri, P. and Canagarajah, N. "Modelling diffusion at the boundary of a digital waveguide mesh" *Proc. Int. Computer Music Conf. (ICMC'99), Beijing, China,* 492-495, 1999.

[4] Kirszenstein, J. "An image source computer model for room acoustics" *Applied Acoustics*, **17**, 275-290, 1984.

[5] Kulowski, A. "Algorithmic representation of the ray-tracing technique" *Applied Acoustics*, **18**, 449-465, 1985.

[6] Vörlander, M. "Simulation of the transient and steady-state sound propagation in rooms using a new combined ray-tracing/image-source algorithm" *J. Acoust. Soc. Am.*, **86**, 172-178, 1989.

[7] Cotana, F. "An improved room acoustic model" *Applied Acoustics*, **61**, 1-25, 2000.

[8] Murphy, D. T. and Howard, D. M. "2D digital waveguide mesh topologies in room acoustics modelling" *Proc. Cost G-6 Conf. Dig. Audio Effects (DAFX-00) Verona Italy,* 211-216, 2000.

[9] O'Connor, W. and Cavanagh, F. "Transmission line matrix acoustic modelling on a PC" *Applied Acoustics*, **50**, 247-255, 1997.

[10] Wilde, A., Eccardt, P-C. and O'Connor, W. "Modeling acoustic transducer surface waves by the TLM method" *Proc. 19th CAD-FEM User's Meeting, Int. Congress FEM Technology, Berlin, Potsdam*, 2001.

[11] Flint, J. A., Goodson, A. D. and Pomeroy, S.C. "Visualising wave propagation in bioacoustic lens structures using the TLM method" *Proc. Inst. Acoustics*, **19**, 29-37, 1997.

[12] Morton, M. *The Transmission Line Matrix Modelling of Signal Propagation within Systems Containing Reflective Boundaries*, MSc. Thesis, School of Information Systems, University of East Anglia, Norwich, 2001.

[13] El-Masri, S., Perolson, X., Saguet, P. and Badin, P. "Vocal tract acoustics using the TLM method" *Proc. Int. Conf. Speech and Language Processing*, 953-956, 1996.

[14] Aird, M, Laird, J. and Ffitch, J. "Modeling a drum by interfacing 2D and 3D waveguide meshes" *Proc. Int. Computer Music Conf. (ICMC'00) Berlin Germany*. 2000.

[15] Van Duyne, S. A. and Smith III, J. O. "The tetrahedral digital waveguide mesh" *Proc. 1995 IEEE Workshop Applic. Signal Processing to Audio & Acoustics*, 1-4, 1995.

[16] Van Duyne, S. A. and Smith III, J. O. "The 3D tetrahedral digital waveguide mesh with musical applications" *Proc. 1996 Int. Computer Music Conf. (ICMC'96), Beijing, China,* 9-16, 1996.

[17] Morente, J. A., Porti, J. A. and Khalladi, M. "Absorbing boundary conditions for the TLM" *IEEE Trans. Microwave Theory Techniques*, **40**, 2095-2099, 1992.

[18] Berenger, J. P. "A perfectly matched layer for the absorption of electromagnetic waves" *J. Comput. Phys.*, **114**, 185-200, 1994.

[19] Miklavic, S. J. and Ninham, B. W. "Conformation of surface bound polyelectrolytes. I" *J. theor. Biol.,* **137**, 71-89, 1989.

[20] Granfeldt, M. K, Miklavic, S. J., Marcelja, S. and Woodward, C. E. "Conformation of surface bound polyelectrolytes. II" *Macromolecules,* **23**, 4760-4768, 1990.

[21] Van Duyne, S. A. and Smith III, J. O. "Physical modeling with the 2D digital waveguide mesh" *Proc. Int. Computer Music Conf. (ICMC'93), Tokyo, Japan,* 40-47, 1993.

[22] Savioja, L. and Välimäki, V. "Interpolated rectangular 3D digital waveguide mesh algorithms with frequency warping" *IEEE Trans. Speech Audio Proc.*, **11**, 783-790, 2003.

[23] Ericsson, J. *Simulation of Room Acoustics using the 3-D Tetrahedral Transmission Line Matrix Method* MSc. Thesis Linköping University, 2004 (ISRN: LITH-ITN-MT-EX-04/021-SE, LiU Press)

[24] Kilgard, M. J. *The Open GL Utility Toolkit (GLUT) Programming Interface API Vers B* (http://opengl.org/documentation/specs/glut/spec3/spec3.html, 1996. Downloaded 21/1-04).